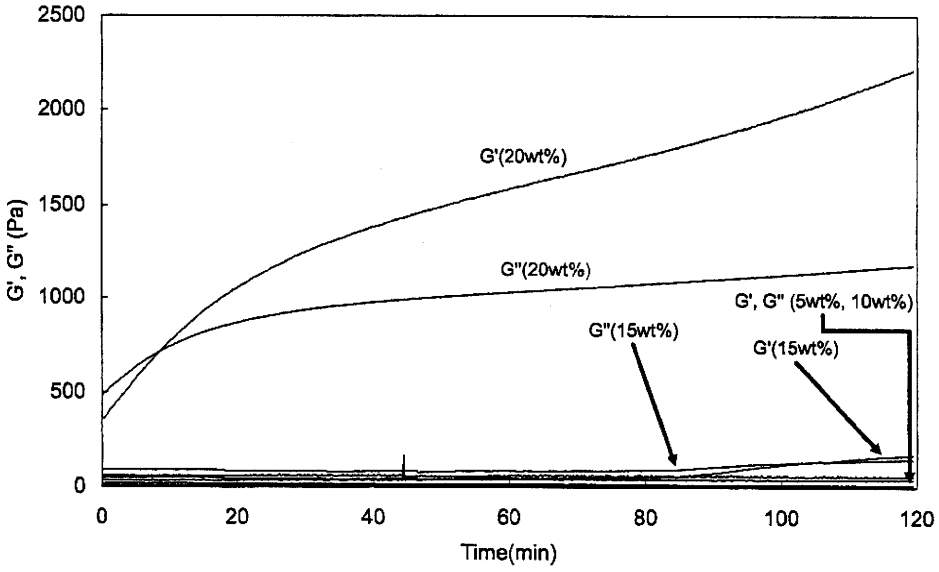

Figure 3. The elastic modulus (G') and viscous modulus (G'') of the mixture of X-PMLLA20-5 and X-PMDLA20-5 solutions with various concentrations.

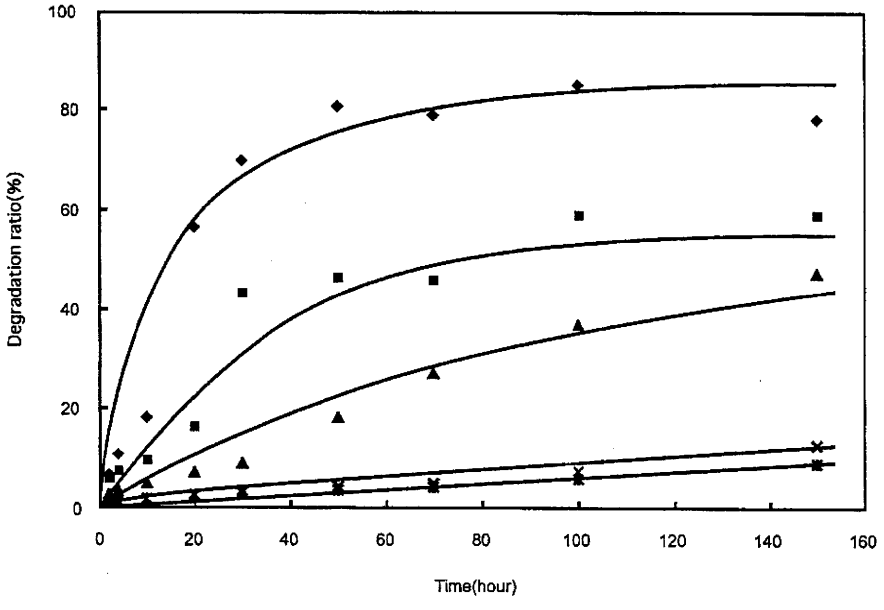

Figure 4. Degradation profile of X-SC gel (X-SC20-10) under various pH conditions. (◆) pH 7.8, (■) pH 7.4, (▲) pH 6.8, (×) pH 6.0 and (*) pH 5.8.

ability of the hydrogel containing FITC-labeled BSA was substantially low due to the high molecular weight of BSA, the increase in fluorescence intensity almost corresponded to the degradation process of the hydrogel. In Fig. 4, the degrada-

tion ratio of the hydrogel, which is evaluated using the fluorescence intensity, is plotted as a function of time and pH. The fluorescence intensity became saturated at conditions corresponding to 100 h, 37°C and pH 7.4. The degradation rate increased in media with a higher pH. The X-SCgel disappeared in the PBS due to hydrolysis of oligo(lactic acid) chains and cross-linking points, which destroyed the stereocomplex. It could be suggested that the X-SCgel degrades under physiological conditions in the body. Furthermore, the main chains remained and were not degraded under physiological conditions; however, these chains are water-soluble polymers. The molecular weight of the main chain was controlled at less than 3.0×10^4. Thus, we consider that these chains can be excreted in urine. From an overall perspective, the results suggest that hydrogels composed of PMLLA and PMDLA can undergo hydrolysis under physiological conditions and that the products can be completely eliminated from the body.

4. Conclusion

To develop an injectable and biocompatible hydrogel system, we synthesized a water-soluble graft polymer composed of MPC and oligo(lactic acid) macromonomer units using living radical polymerization. These polymers underwent spontaneous gelation due to the formation of a stereocomplex between the racemates of oligo(lactic acid) macromonomer units in an aqueous medium. The properties of the hydrogel depended on the concentration of the polymers. The hydrogels degraded in a buffer solution by hydrolysis of the side chain, and the degradation products dissolved in the buffer solution. From these results, it is suggested that the polymer system could be applied as an injectable, biocompatible, and degradable hydrogel system to serve as a reservoir of bioactive molecules in drug-delivery systems and as a scaffold in cell-based tissue engineering.

Acknowledgements

The authors thank Associate Professor Tomohiro Konno, Dr. Ryosuke Matsuno and Dr. Yuuki Inoue, all from The University of Tokyo, for their valuable inputs. This study was partially supported by Core Research for Evolution Science and Technology (CREST), Japan Science and Technology Agency.

References

1. N. A. Peppas, *Hydrogels in Medicine and Pharmacy, Vol. III: Properties and Applications*. CRC Press, Boca Raton, FL (1987).
2. C. He, S. W. Kim and D. S. Lee, *J. Control. Rel.* **127**, 189 (2008).
3. A. Gutowska, B. Jeong and M. Jasionowski, *Anat. Rec.* **263**, 342 (2001).
4. S. J. de Jong, W. N. E. van Dijk-Wolthuis, J. J. Kettenes-van den Bosch, P. J. W. Schuyl and W. E. Hennink, *Macromolecules* **31**, 6397 (1998).
5. S. J. de Jong, S. C. De Smedt, M. W. C. Wahls, J. Demeester, J. J. Kettenes-van den Bosch and W. E. Hennink, *Macromolecules* **33**, 3680 (2000).

6. S. J. de Jong, B. van Eerdenbrugh, C. F. van Nostrum, J. J. Kettenes-van den Bosch and W. E. Hennink, *J. Control. Rel.* **71**, 261 (2001).
7. H. Tsuji, F. Horii, S. Hyon and Y.Ikada, *Macromolecules* **24**, 2719 (1991).
8. T. Fujiwara, T. Mukose, T. Yamaoka, H. Yamane, S. Sakurai and Y. Kimura, *Macromol. Biosci.* **1**, 204 (2001).
9. S. M. Li, A. El Ghzaoui and E. Dewinck, *Macromol. Symp.* **222**, 23 (2005).
10. S. M. Li and M. Vert, *Macromolecules* **36**, 8008 (2003).
11. J. Watanabe, T. Eriguchi and K. Ishihara, *Biomacromolecules* **3**, 1109 (2002).
12. J. Watanabe, T. Eriguchi and K. Ishihara, *Biomacromolecules* **3**, 1375 (2002).
13. K. Ishihara, R. Aragaki, T. Ueda, A. Watanabe and N. Nakabayashi, *J. Biomed. Mater. Res.* **24**, 1069 (1990).
14. K. Ishihara, N. P. Ziats, B. P. Tierney, N. Nakabayashi and J. M. Anderson, *J. Biomed. Mater. Res.* **25**, 1397 (1991).
15. K. Ishihara, H. Oshida, T. Ueda, Y. Endo, A. Watanabe and N. Nakabayashi, *J. Biomed. Mater. Res.* **26**, 1543 (1992).
16. K. Ishihara, T. Tsuji, Y. Sakai and N. Nakabayashi, *J. Polym. Sci. Part A: Polym. Chem.* **32**, 859 (1994).
17. K. Ishihara, H. Nomura, T. Mihara, K. Kurita, Y. Iwasaki and N. Nakabayashi, *J. Biomed. Mater. Res.* **39**, 323 (1998).
18. S. Sawada, S. Sakaki, Y. Iwasaki, N. Nakabayashi and K. Ishihara, *J. Biomed. Mater. Res. A* **64**, 411 (2003).
19. K. Ishihara, E. Ishikawa, A. Watanabe, Y. Iwasaki, K. Kurita and N. Nakabayashi, *J. Biomater. Sci. Polymer Edn* **10**, 1047 (1999).
20. S. Kihara, K. Yamazaki, K. N. Litwak, P. Litwak, M. V. Kameneva, H. Ushiyama, T. Tokuno, D. C. Borzelleca, M. Umeda, J. Tomioka, O. Tagusari, T. Akimoto, H. Koyanagi, H. Kurosawa, R. L. Kormos and B. P.Griffith, *Artif. Organs* **27**, 188 (2003).
21. M.Sakakida, K. Nishida, M. Shichiri, K. Ishihara and N. Nakabayashi, *Sensors Actuators* **13–14**, 319 (1993).
22. X. Xu, X. Chen, Z. Wang and X. Jing, *Eur. J. Pharm.* **72**, 18 (2009).
23. K. Hu, J. Li, Y. Shen, W. Lu, X. Gao, Q. Zhang and X. Jiang, *J. Control. Rel.* **134**, 55 (2009).
24. K. Ishihara, T. Ueda and N. Nakabayashi, *Polym. J.* **22**, 355 (1990).
25. T. Ueda, H. Oshida, K. Kurita, K. Ishihara and N. Nakabayashi, *Polym. J.* **24**, 1259 (1992).
26. T. Otsu and A. Kuriyama, *Polym. Bull.* **11**, 135 (1984).
27. D. W. Lim, S. Choi and T. G. Park, *Macromol. Rapid Commun.* **21**, 464 (2000).
28. A. L. Lewis, *Colloids Surface B: Biointerfaces* **18**, 261 (2000).
29. Y. Iwasaki and K. Ishihara, *Anal. Bioanal. Chem.* **381**, 534 (2005).
30. K. Ishihara and M. Takai, *J. Roy. Soc. Interface* **6** (Suppl.), S279 (2009).
31. T. Goda and K. Ishihara, *Expert. Rev. Med. Devices* **3**, 167 (2006).
32. M. Kimura, M. Takai and K. Ishihara, *J. Biomed. Mater. Res. A* **80**, 45 (2007).
33. M. Kimura, M. Takai and K. Ishihara, *J. Biomater. Sci. Polym. Edn* **18**, 623 (2007).

Biomaterials 32 (2011) 2241–2247

Contents lists available at ScienceDirect

Biomaterials

journal homepage: www.elsevier.com/locate/biomaterials

Tissue response to poly(L-lactic acid)-based blend with phospholipid polymer for biodegradable cardiovascular stents

Hyung Il Kim [a,b,h,i], Kazuhiko Ishihara [a,b,c,i,*], Seungbok Lee [d,e], Ji-Hun Seo [c,i], Hye Young Kim [f], Dongwhan Suh [d,e], Min Uk Kim [g], Tomohiro Konno [a,i], Madoka Takai [c], Jeong-Sun Seo [d,e,h,**]

[a] Department of Bioengineering, School of Engineering, The University of Tokyo, 7-3-1, Hongo, Bunkyo-ku, Tokyo 113-8656, Japan
[b] Center for Medical System Innovation, The University of Tokyo, Hongo, Bunkyo-ku, Tokyo 113-8656, Japan
[c] Department of Materials Engineering, School of Engineering, The University of Tokyo, Hongo, Bunkyo-ku, Tokyo 113-8656, Japan
[d] Department of Biomedical Sciences, Genomic Medicine Institute, Seoul National University College of Medicine, Seoul 110-799, Republic of Korea
[e] Department of Biochemistry and Molecular Biology, Genomic Medicine Institute, Seoul National University College of Medicine, Seoul 110-799, Republic of Korea
[f] Department of Anesthesiology and Pain Medicine, Seoul National University Hospital, Seoul 110-744, Republic of Korea
[g] Department of Radiology, Seoul National University Hospital, Seoul 110-744, Republic of Korea
[h] Macrogen Inc., Seoul 153-023, Republic of Korea
[i] Core Research for Evolutional Science and Technology (CREST), Japan Science and Technology Agency, 5 Sanban-cho, Chiyoda-ku, Tokyo 102-0075, Japan

ARTICLE INFO

Article history:
Received 28 September 2010
Accepted 27 November 2010
Available online 24 December 2010

Keywords:
Polymer blend
poly(lactic acid)
Phosphorylcholine group
Tissue compatibility
Cardiovascular stent

ABSTRACT

A temporary cardiovascular stent device by bioabsorbable materials might reduce late stent thrombosis. A water-soluble amphiphilic phospholipid polymer bearing phosphorylcholine groups (PMB30W) was blended with a high-molecular-weight poly(L-lactic acid) (PLLA) to reduce unfavorable tissue responses at the surface. The PLLA implants and the polymer blend (PLLA/PMB30W) implants were inserted into subcutaneous tissues of rats, the infrarenal aorta of rats, and the internal carotid arteries of rabbits. After 6 months subcutaneous implantation, the PLLA/PMB30W maintained high density of phosphorylcholine groups on the surface without a significant bioabsorption. After intravascular implantation, the cross-sectional areas of polymer tubing with diameters less than 1.6 mm were histomorphometrically measured. Compared to the PLLA tubing, the PLLA/PMB30W tubing significantly reduced the thrombus formation during 30 d of implantation. Human peripheral blood mononuclear cells were cultured on the PLLA and the PLLA/PMB30W to compare inflammatory reactions. Enzyme-linked immunosorbent assay quantified substantially decreased proinflammatory cytokines in the case of the PLLA/PMB30W. They were almost the same level as the negative controls. Thus, we conclude that the phosphorylcholine groups could reduce tissue responses significantly both in vivo and in vitro, and the PLLA/PMB30W is a promising material for preparing temporary cardiovascular stent devices.

1. Introduction

The treatment of coronary artery disease and other cardiovascular diseases has been revolutionized through the introduction of interventional procedures and the use of intravascular stents, which are inserted by a minimally invasive method and mechanically scaffold the vessel wall against elastic recoil, improving blood flow in diseased vessels [1,2]. However, current drug-eluting stents permanently remain in implantation sites with several limitations, including the risks of late stent thrombosis, hindrance of late lumen vessel enlargement, and interference with radiological imaging [3]. High-molecular-weight poly(L-lactic acid) (PLLA) has the potential to replace permanent stenting and has exhibited favorable degradation behavior in small clinical trials [3–5]. The PLLA is a biodegradable polymer whose molecular weight decreases over time due to cleavage of the ester linkage, degrading into small particles that can be phagocytosed [3,4]. Eventually, the PLLA is degraded into lactic acid and is eliminated through the citric acid cycle.

Safety concerns regarding the use of the PLLA for stenting remain, however, because foreign materials are inherently

* Corresponding author. Department of Bioengineering, School of Engineering, University of Tokyo, Tokyo 113-8656, Japan. Tel.: +81 3 5841 7124; fax: +81 3 5841 8647.
** Corresponding author. Department of Biomedical Sciences, Genomic Medicine Institute, Seoul National University College of Medicine, Seoul 110-799, Republic of Korea. Tel.: +82 2 740 8246; fax: +82 2 741 5423.
E-mail addresses: ishihara@mpc.t.u-tokyo.ac.jp (K. Ishihara), jeongsun@snu.ac.kr (J.-S. Seo).

0142-9612/$ – see front matter © 2010 Elsevier Ltd. All rights reserved.
doi:10.1016/j.biomaterials.2010.11.067

thrombogenic [6–11]. This is attributed to the denaturation of proteins, activation of coagulation factors, propagation of thrombi, provocation of inflammatory responses, and accumulation of debris. To control these adverse tissue reactions on the materials, the surface of the materials was covered with phosphorylcholine groups for preparing artificial cell membrane without any ligand molecules. Based on this hypothesis, 2-methacryloyloxyethyl phosphorylcholine (MPC) copolymers, which have phosphorylcholine groups in their side chain, have been synthesized [12–17]. The MPC copolymers can be incorporated by a convenient procedure such as blending with matrix polymers [18–21]. In a molecular and mechanistic approach, the biomedical function of the MPC copolymers has been explained by the free water fraction on the surface, which minimizes protein adsorption and its conformational change [22–24]. Surfaces of materials with a high density of phosphorylcholine groups significantly lower platelet activation and neointimal hyperplasia [25–30]. A water-soluble poly[MPC-*co*-*n*-butyl methacrylate (BMA)] (PMB30W) is an amphiphilic copolymer composed of hydrophobic BMA units and hydrophilic MPC units [12,13,31]. Due to its strong amphiphilic characteristics, the PMB30W plays a dual role as a biomimetic modifier of surface properties and as a surfactant for the bulk properties of polymer blends composed of PLLA and PMB30W (PLLA/PMB30W) [11].

Although it has been presumed that phosphorylcholine groups on the surface of materials can enhance biocompatibility, the critical concept that the incorporation of phosphorylcholine groups might reduce stent thrombosis has not been resolved in vitro [32], preclinically [33], or clinically [34]. This discrepancy may be due to the different dispersion state of phosphorylcholine groups on the surfaces of stent materials [11,14–17,32,33]. In the present study, we hypothesized that the PLLA/PMB30W with phosphorylcholine group-rich surfaces could exhibit favorable bulk and surface properties in vivo and may enhance tissue compatibility of temporary cardiovascular stent devices. Therefore, the objective of this study was comparison of tissue responses on the PLLA/PMB30W and the PLLA in vivo with small animal models and in vitro, and to discuss the role of the phosphorylcholine groups for reducing the tissue responses.

2. Materials and methods

2.1. Preparation of materials

The PLLA (molecular weight (Mw) = 1×10^5 for the preparation of tubing or Mw = 5×10^4 for the preparation of films) was purchased from Polysciences, Warrington, PA. The PMB30W was synthesized using a free radical polymerization technique by a previously reported method [12,13,31]. The chemical structure of PMB30W is shown in Fig. 1. The PMB30W concentrations >1 mg/mL in phosphate-buffered saline (PBS) result in the PMB30W nanoaggregates with hydrodynamic diameters <20 nm [31,35].

The PLLA and the PLLA/PMB30W (weight ratio, 92/8) tubing and films were prepared by a modified previously reported method [11]. Briefly, 6 wt% PLLA solution in dichloromethane (DCM)/methanol (MeOH) (volume ratio, 12/1) and 6 wt% PLLA/PMB30W (weight ratio, 92/8) solution in DCM/MeOH (volume ratio, 12/1) were repeatedly coated onto Teflon® rods (tubing) or cast onto Teflon® dishes (films), and the solvents were dried at room temperature. Polymer tubing and films were vacuum-dried for 1 week, and then immersed in water to equilibrate the surface overnight before the surface measurements. Polymer tubing and films were sterilized with ethylene oxide gas at 40 °C.

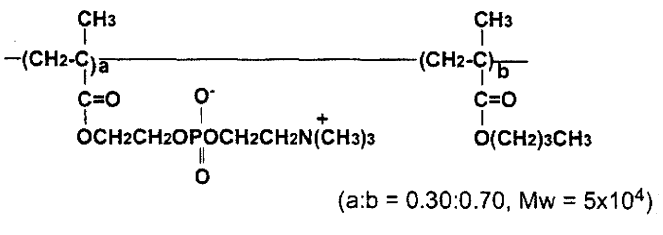

Fig. 1. The chemical structure of the PMB30W.

2.2. Surface characteristics of materials

To analyze the inner surface of polymer implants, the tubing was cut into concave membranes and pressed under 50 MPa at 60 °C for 10 min. The atomic concentration on the inner surface was measured using an X-ray photoelectron spectroscope (XPS; AXIS-HSi, Kratos/Shimadzu, Kyoto, Japan) with a magnesium Kα (energy = 1253.6 eV) source radiation. The photoelectron take-off angle was 90°. The measured phosphorous atomic concentration was attributed to the phosphorus in the phosphorylcholine groups of the PMB30W. The phosphorous/carbon atomic concentration ratios (P/C% values) were calculated by determining the relevant integral peak area and applying the sensitivity factors supplied by the instrument manufacturer (Supplementary Fig. 1).

To measure the static contact angle (SCA), a captive-bubble method was used. The polymer films were fixed horizontally, and a small air bubble was attached to the mold contact surface of polymer films in the distilled water and the SCA in water was determined by the angle between the films and the air bubble using a contact angle goniometer (CA-W, Kyowa, Saitama, Tokyo, Japan) at room temperature.

2.3. Evaluation of bioabsorption of polymer implants after subcutaneous implantation

Animal care and procedures were approved by Institutional Animal Care and Use Committee (IACUC) (No. 080929-3) at Seoul National University. The PLLA (n = 15) and PLLA/PMB30W (n = 15) polymer tubing (internal diameter [ID]: 1.6 mm; thickness: 0.2 mm; length: 2.5 cm) was implanted into the interscapular subcutaneous tissue of rats (n = 30, male Wistar, body weight: 0.3–0.4 kg) after anesthesia by inhalation of 2% isoflurane. At predetermined times (2, 4, 6 months), the polymer tubing was explanted after the animals were euthanized. The fibrous capsule surrounding the tubing was carefully removed. The polymer tubing was sonicated in 1% sodium dodecyl sulfate aqueous solution for 20 min to remove the adsorbed components and rinsed with distilled water. After vacuum drying, changes in the overall mass and molecular weight of the polymer tubing were calculated by a gravimetric method and gel permeation chromatography (Jasco system, Tokyo, Japan), respectively. The polymer tubing was dissolved in 1,1,1,3,3,3-hexafluoroisopropanol; the flow was 0.2 mL/min at 40 °C. The molecular weight of polymer was calibrated by poly(methyl methacrylate) standards.

2.4. Evaluation of acute thrombus formation after intravascular tubing insertion into small animals

Animal care and procedures were approved by IACUC (No. 08-0266) at Seoul National University Hospital.

Wistar male rats (n = 17, body weight: 0.3–0.4 kg) were anesthetized by inhalation of 2% isoflurane. After the infrarenal abdominal aorta of each animal was surgically exposed and clipped by an approximator with a surgical microscope, the vessels were carefully punctured using a taper-point needle. Then, polymer tubing (n = 17; ID: 1.2 mm; thickness: 150 μm; length: 2.0 mm) was inserted using a 20 G catheter, and the puncture sites were sutured with Ethilon 10-0 as described in Results.

For paired tests, New Zealand white male rabbits (n = 11, body weight: 3–4 kg) were anesthetized by intramuscular injection of a mixture of Zoletil (15 mg/kg) and xylazine (7.5 mg/kg) and subsequent inhalation of nitric oxide and isoflurane. Heparin (50 IU/kg per h) was administered to the rabbits as a continuous infusion during the operative procedure. With a surgical microscope, each internal carotid artery was carefully exposed and clipped by an approximator. After puncturing vessels by the aforementioned method, the polymer tubing (n = 22; ID: 1.6 mm; thickness: 150 μm; length: 3.0 mm) was inserted using an 18 G catheter. The PLLA tubing (n = 11) was inserted into the left internal carotid arteries, and the PLLA/PMB30W tubing (n = 11) was inserted into the right internal carotid arteries. The puncture sites were then sutured with Ethilon 8-0.

At predetermined times (3 h and 30 d in the rat study; 2 d and 30 d in the rabbit study), the polymer tubing-inserted arteries were surgically explanted after a heparin injection (200 IU/kg), following which the animals were euthanized. The samples were then rinsed with normal saline, placed in 2.5% glutaraldehyde PBS solution overnight, rinsed with distilled water, embedded in optimal cutting temperature compound, and cross-sectioned (thickness: 0.30 mm) while in a deep frozen state. The frozen sections were prepared by an independent researcher. For morphometric analysis, all cross-sections [PLLA from rats at 3 h (n = 13), PLLA/PMB30W from rats at 3 h (n = 12), PLLA from rats at 30 d (n = 8), PLLA/PMB30W from rats at 30 d (n = 10), PLLA from rabbits at 2 d (n = 26), PLLA/PMB30W from rabbits at 2 d (n = 20), PLLA from rabbits at 30 d (n = 32), PLLA/PMB30W from rabbits at 30 d (n = 29)] were digitally exported from a microscope camera, and the patent cross-sectional area (CSA) was analyzed using the National Institutes of Health ImageJ software (version 1.41o). Lumen area stenosis (LAS) was calculated as $[1.00 - (S/T)] \times 100$, where T is the CSA of the unimplanted polymer tubing, and S is the minimal CSA of each polymer tubing-inserted artery. In the rat study, T = 1.13 mm^2, and in the rabbit study, T = 2.01 mm^2. For observation of vessel remodeling, a PLLA/PMB30W-inserted aorta of rat (n = 1) after 50 d of implantation

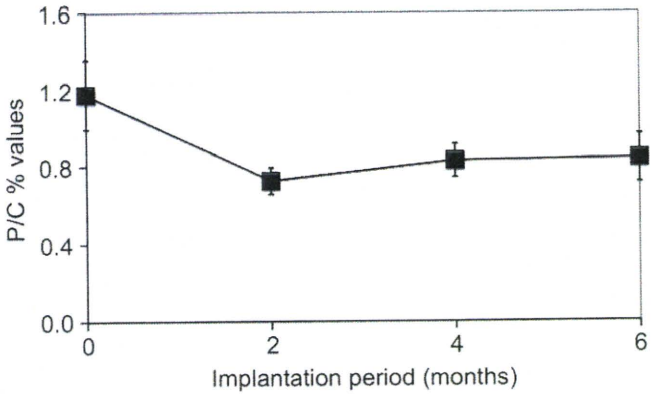

Fig. 2. Surface characteristics of the PLLA/PMB30W over 6 months of subcutaneous implantation. The P/C% values of the inner surface of the PLLA/PMB30W tubing (n = 4–5 implants per time point) were measured by X-ray photoelectron spectroscopy.

was embedded with acrylic resin. The cross-sections were prepared by a standard microtome and stained with hematoxylin-eosin.

2.5. Evaluation of proinflammatory cytokines released form human peripheral blood mononuclear cells during contact with polymer films

Human peripheral blood mononuclear cells (hPBMCs) from a single healthy donor were purchased from Lonza (Basel, Switzerland). The hPBMCs were incubated in RPMI-1600 with 10% FBS, 100 units/mL penicillin, 100 μg/mL streptomycin, 2 mM glutamine, 40 units/mL DNase, and 70 ng/mL G-CSF on commercially available 12-well polystyrene plates treated with an MPC polymer (Nunc Japan, Tokyo, Japan) with and without the PLLA or the PLLA/PMB30W films (diameter: 20 mm, thickness: 0.2 mm) at densities of 2.0×10^6 hPBMCs per well. The mold contact surface of polymer films was placed upward. At 24 h, supernatants were collected after centrifugation at 200 × g for 15 min. Then, the hPBMCs were incubated in fresh medium. The supernatants were collected 48 h after centrifugation at 200 × g for 15 min. Commercially available kits based on the enzyme-linked immunosorbent assay (ELISA) (R&D Systems, Minneapolis, MN) were employed for the quantitative determination of macrophage migration inhibitory factor (MIF), monocyte chemoattractant protein-1 (MCP-1), interleukin 1β (IL-1β), IL-6, and tumor necrosis factor-α (TNF-α). Each standard and sample was tested in duplicate; samples that have a variation coefficient >0.20 were remeasured. The absorbance of each sample was recorded using a microplate reader after the blank subtraction that corrects optical imperfections in the plate.

2.6. Statistical analysis

Data are expressed as means and standard deviations. Statistical differences ($^*P < 0.05$; $^{**}P < 0.01$; $^{***}P < 0.001$) were analyzed by the Mann–Whitney U test for the animal studies and the analysis of variance (ANOVA) with the Bonferroni correction for the in vitro study.

3. Results and discussion

3.1. Bioabsorption of polymer implants after subcutaneous implantation

The subcutaneous milieu is considered adequate for evaluation of the basic properties of cardiovascular implants, such as biodegradation [36]. Rapid biodegradation of temporary stent materials could lead to incomplete opposition to vessel recoil forces [3–5]. Over the 6-month observation period, weight loss of both PLLA and PLLA/PMB30W was about 2% and the average molecular weight of the PLLA and that of the PLLA/PMB30W still remained over 93% of the initial values (Supplementary Fig. 2). During biodegradation, the changing molecular weight of the PLLA precedes its mass change and determines its bulk properties [11,37]. Because the molecular weight of the PLLA and the PLLA/PMB30W was not changed substantially, it is assumed that the mechanical strengths of the PLLA or those of the PLLA/PMB30W remain unaltered over 6 months of subcutaneous implantation.

The PMB30W is a water-soluble polymer and can be eluted from the surface of implants. However, we previously demonstrated that the tightly entangled blend system of the PLLA/PMB30W did not exhibit a substantial loss of the PMB30W on the surface of tubing during PBS incubation [11]. Fig. 2 shows that the density of phosphorylcholine groups on the inner surface of the PLLA/PMB30W eventually approached equilibrium (the P/C% values = 0.8 ± 0.1) between hydrophilic attraction from the in vivo environment and hydrophobic molecular entanglement with the PLLA chains. These results suggest that the PLLA/PMB30W maintained stable bulk and surface properties during 6 months implantation in vivo.

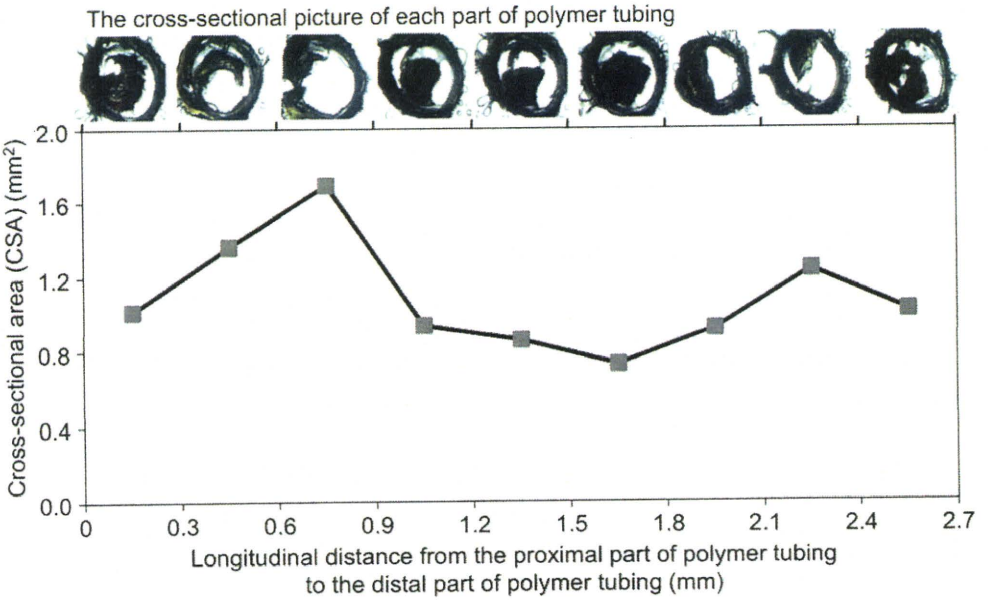

Fig. 3. Analysis of the cross-sectional areas (CSA) of the PLLA/PMB30W tubing after 30 d implantation into an internal carotid artery of a rabbit. After the explanation of the polymer tubing, they were cross-sectioned (thickness: 0.30 mm) while in a deep frozen state. For morphometric analysis, all cross-sections were digitally exported from a microscope camera as shown in the above the figure, and the CSA was calculated using the National Institutes of Health ImageJ software.

Table 1
Cross-sectional areas (CSA) of polymer tubing after implantation into the infrarenal aorta of rats. The CSA of the unimplanted polymer tubing (T) was 1.13 mm^2.

	Number of implants	Implantation period	Mean CSA (mm^2)	Minimal CSA (S) (mm^2)	Lumen area stenosis (%) [{1.00 − (S/T)} × 100]
PLLA	3	3 h	0.14 ± 0.05	0.05 ± 0.05	95.7 ± 4.5
PLLA/PMB30W	3	3 h	0.48 ± 0.03	0.30 ± 0.14	73.3 ± 13.7
PLLA	3	30 d	0.27 ± 0.12	0.23 ± 0.14	79.3 ± 12.5
PLLA/PMB30W	4	30 d	0.66 ± 0.27	0.48 ± 0.20	61.6 ± 21.4

3.2. Acute thrombus formation after intravascular tubing insertion

The procedure of intravascular tubing insertion into small animals has been employed and modified for the evaluation of blood clot formation on the polymer tubing [38]. Because the diameter of the tubing was larger than that of the arteries in which they were implanted and the tubing fully covered the vessel lumen (Supplementary Fig. 3), incomplete apposition was not observed. All polymer implants had identical morphology; any thrombus in the implanted arteries was deposited on the surface of the materials, and CSAs of polymer tubing represent the patent lumen areas as shown in Fig. 3. In our animal models, the vessel wall, which is a compartment rich in tissue factors, was disrupted by puncturing the vessels. Simultaneously, exposed collagen and foreign materials triggered the accumulation and activation of platelets [9]. To focus on material-associated thrombosis, no antithrombotics, except heparin, were administered to the animals. Thus, thrombi were rapidly formed and propagated into the polymer implants, of which the distal part was located approximately 2 mm proximal to the puncture site. This rapid and extensive thrombus formation in small-diameter (<2 mm) vessels can be correlated with frequent failure of small-diameter (<6 mm) vascular prostheses.

Three out of 10 rats in the 30 d groups (PLLA at 1 d, PLLA at 3 d, PLLA/PMB30W at 1 d) died following bilateral lower extremity paralysis due to the occlusion of abdominal aorta and were excluded from further comparisons (Supplementary Fig. 4). Table 1 shows the unpaired comparison of the CSA of the lumens of the PLLA versus those of the PLLA/PMB30W tubing after implantation into the infrarenal aorta of rats. At 3 h after implantation, the averages of mean and minimal CSA of the PLLA versus the PLLA/PMB30W tubing were 0.14 mm^2 versus 0.48 mm^2 and 0.05 mm^2 versus 0.30 mm^2, respectively. At 30 d after implantation, the corresponding values were 0.27 mm^2 versus 0.66 mm^2 and 0.23 mm^2 versus 0.48 mm^2, respectively.

One out of 5 rabbits in the 2 d group was euthanized because the animal was unable to move and suffered from loss of brain function after the surgery. Additionally, 1 out of 6 rabbits in the 30 d group was diagnosed with an infection and euthanized. Table 2 shows the paired comparison of the CSAs of the PLLA versus the PLLA/PMB30W tubing after the materials were implanted into the internal carotid arteries of the rabbits. At 2 d after implantation, the averages of mean and minimal CSA of the PLLA versus the PLLA/PMB30W tubing were 0.38 mm^2 versus 0.88 mm^2 and 0.15 mm^2 versus 0.55 mm^2, respectively. At 30 d, the corresponding values were 0.55 mm^2 versus 0.93 mm^2 and 0.26 mm^2 versus 0.66 mm^2, respectively.

The averages of the total CSA (CSAs overall of the cross-sections) of the PLLA versus the PLLA/PMB30W after implantation into infrarenal aorta of rats were 0.18 mm^2 ($n = 13$) versus 0.49 mm^2 ($n = 12$) ($P = 0.0002$) at 3 h and 0.24 mm^2 ($n = 8$) versus 0.67 mm^2 ($n = 10$) ($P = 0.0019$) at 30 d (Fig. 4A). The corresponding values after implantation into internal carotid artery of rabbits were 0.37 mm^2 ($n = 26$) versus 0.84 mm^2 ($n = 20$) ($P < 0.0001$) at 2 d and 0.59 mm^2 ($n = 32$) versus 0.96 mm^2 ($n = 29$) ($P < 0.0001$) at 30 d (Fig. 4B).

Considering that thrombosis was initiated in vulnerable areas, thrombus propagation on the stent materials would depend on platelet deposition, accumulation of tissue factors, and generation of fibrin [9,10]. The surfaces containing high density of phosphorylcholine groups have the free water fraction and could reduce the thrombus formation [22–24]. During the remodeling process, the thrombus slowly regressed over time. The remaining thrombus volume provided a provisional matrix [7] into which smooth muscle cells migrated, proliferated, and synthesized extracellular matrix (Fig. 5). The remarkable thrombus formation on polymer implants was presumably due to the short distance (~2 mm) between the puncture site and the implantation site. Further, no antithrombotics (except heparin in the rabbit study) were administered, which is different from the real clinical situation. Thus, significantly different levels of thrombus formation were observed between the PLLA and the PLLA/PMB30W.

Intravascular tubing insertion has several merits for the exploration of blood-stent material interactions; a uniformly circular lumen shape of stent materials could control vascular responses [39], and CSA can be obtained by simple objective histomorphometry. In contrast, in vitro tests of thrombogenicity hinder the full range of interactions among platelets, complementary systems, and cellular components and produce inevitable artifacts of the blood–air interaction and of blood with other substrates; such systems are thus generally incapable of predicting in vivo performance [40]. In the present study, the in vivo inflammatory reaction has not been compared because the polymers showed brittleness on a standard microtome and elongation in the acrylic resin embedding. Moreover, the mechanical injury caused by the rigid scaffolds and surgical procedures could mask the inflammatory reaction of tissues contacting materials in both subcutaneous and intravascular implantation. For these reasons, thick frozen cross-sections (thickness: 0.30 mm) were primarily prepared for histomorphometric measurements (See Fig. 3).

3.3. Proinflammatory cytokines released form human peripheral blood mononuclear cells during contact with polymer films

Although thrombus formation and the inflammatory reaction are interconnected [40–42], inflammation without acute thrombosis

Table 2
Cross-sectional areas (CSA) of polymer tubing after implantation into the internal carotid arteries of rabbits. The CSA of the unimplanted polymer tubing (T) was 2.01 mm^2.

	Number of implants	Implantation period	Mean CSA (mm^2)	Minimal CSA (S) (mm^2)	Lumen area stenosis (%) [{1.00 − (S/T)} × 100]
PLLA	4	2 d	0.38 ± 0.08	0.15 ± 0.11	92.3 ± 5.4
PLLA/PMB30W	4	2 d	0.88 ± 0.41	0.55 ± 0.30	72.8 ± 15.0
PLLA	5	30 d	0.55 ± 0.28	0.26 ± 0.11	87.1 ± 5.7
PLLA/PMB30W	5	30 d	0.93 ± 0.16	0.66 ± 0.19	67.2 ± 9.2

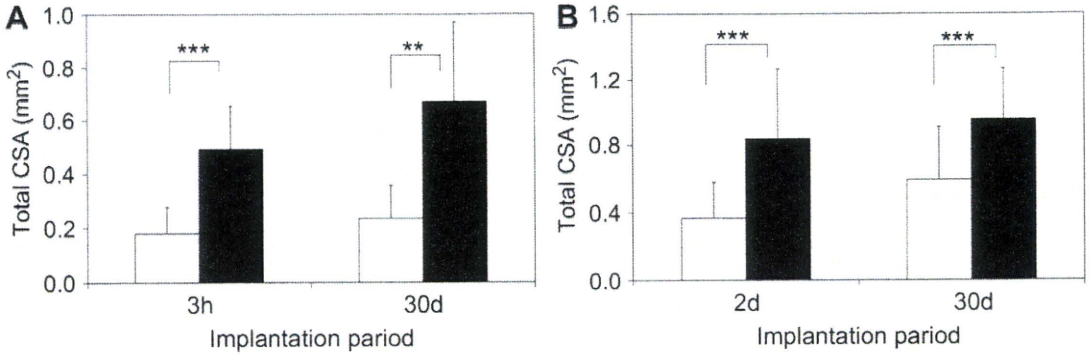

Fig. 4. Comparison studies of the CSA in the PLLA (open column) and the PLLA/PMB30W (closed column) after intravascular implantation into (A) the infrarenal aorta of rats and (B) the internal carotid arteries of rabbits. The *P* values were obtained by the Mann–Whitney *U* test.

can occur and trigger restenosis. Since acute thrombosis has been reduced by the evolution of surgical procedures and antithrombotics, chemokines expressed from a variety of cells, such as neutrophils and monocytes, have become more relevant to the chronic responses toward biomaterials [41]. Thus, inflammatory cytokines of hPBMCs were evaluated after contact with the PLLA films, the PLLA/PMB30W films, or no-polymer films.

The PLLA/PMB30W films have a moderately hydrophilic surface (SCA = 35 ± 8°), while the PLLA films are hydrophobic (SCA = 61 ± 8°). Because hydrophilic phosphorylcholine groups may rearrange at the water interface in an aqueous environment, a captive-bubble method was employed to determine SCA. The P/C % values of the mold contact surface of the PLLA/PMB30W films reached 1.33 after overnight incubation in water.

Fig. 6 shows concentrations of proinflammatory cytokines from hPBMCs cultured with and without polymer films. (The numerical data are available in Supplementary Table 1.) The MIF is considered to be a key player in the inflammatory reaction and in cardiovascular disease, and may play a proximal role in the hierarchy of cytokines [43]. Monocytes play a critical role in defense against foreign organisms and in regulating the behavior of other cells. The MCP-1 is thought to be responsible for monocyte recruitment in acute and chronic inflammation [44]. The acute phase cytokines IL-1β, IL-6, and TNF-α are produced early during inflammatory processes in cardiovascular tissue [45]. Thus, MIF, MCP-1, IL-1β, IL-6, and TNF-α in hPBMCs were quantified after contact with materials.

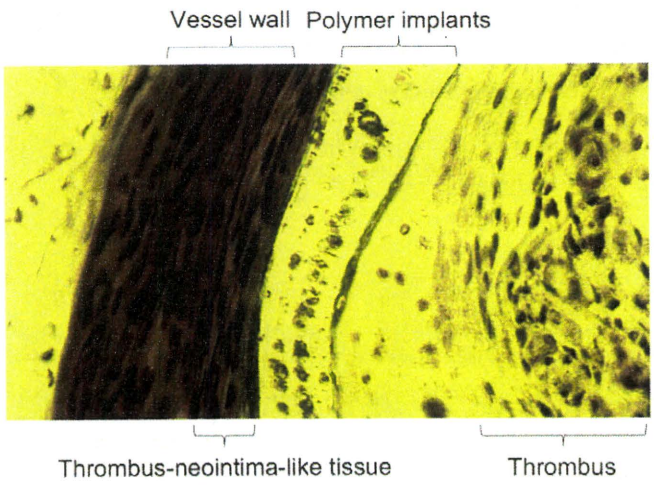

Fig. 5. A vessel remodeling after the intravascular tubing insertion. A cross-section of the polymer tubing-inserted artery at 50 d shows thrombus-neointima-like tissues leading to apposition of polymer implants, and the thrombus remained on the inner surface of the polymer implant. The polymer was elongated during embedding with acrylic resin. Smooth muscle cells proliferated into the thrombotic matrix.

Compared to the PLLA, the PLLA/PMB30W stimulated less robust proinflammatory cytokine activation. Although high concentrations of the MIF were observed in all groups at 1 d, the MIF concentrations were lowest on the no-polymer film (negative control) and were highest on the PLLA at 3 d. The high MIF expression observed at 1 d could be due to the freezing and thawing of hPBMCs before contact with the materials. At 1 d, both the PLLA and the no-polymer film induced high concentrations of MCP-1 compared with that induced by the PLLA/PMB30W. At 3 d, the no-polymer film amplified MCP-1 production while the PLLA and the PLLA/PMB30W did not. The amplification of MCP-1 production on the no-polymer film can be explained as a danger signal for surviving monocytes. Hydrophilic substrates increase the proportion of adherent apoptotic monocytes/macrophages [46], and hydrophilic phosphorylcholine groups contribute to suppressing monocyte adhesion on the surfaces of materials [47,48]. However, the generation of cytokines by monocytes is not proportional to the number of cells adherent to the surface [49]. Here, high MCP-1 expression represents a double-edged survival strategy, protecting cells from apoptosis and enabling them to migrate toward targets [50]. In an optical examination, clustered hPBMCs were observed on no-polymer film, but not on polymer film. This suggests that the cell–cell interaction was far more significant on extremely hydrophilic substrates [51]. Although it is clear that the lowest expression of MCP-1 on the PLLA/PMB30W films indicates monocyte quiescence, this may be interpreted with caution, when compared to the no-polymer film. In vivo, monocytes have a universal chance to migrate toward other sites unlike in vitro culture, where the cells make permanent contact with the hydrophilic surface and confront hydrophilic apoptosis. Concentrations of IL-1β and IL-6 were substantially different on the PLLA and the PLLA/PMB30W at 1 d. At 3 d, concentrations of IL-1β and IL-6 on the PLLA/PMB30W and on the no-polymer film were below detection limits, while those on the PLLA were increased (data not shown). The release of TNF-α stimulated by the PLLA and the PLLA/PMB30W was significantly different at 1 and 3 d. Relatively high expression of TNF-α could be due to administration of G-CSF into the culture medium, although other reports have previously described discrepancies in the expression of TNF-α and IL-1β by hPBMCs [52]. The mechanism that evokes the inflammatory reaction of hPBMCs to biomaterials has yet to be elucidated [41]. Monocyte inactivation on hydrophilic substrates prevents differentiation of macrophages [46], but the apoptosis of healthy monocytes does not guarantee cytocompatibility.

The surfaces covered with phosphorylcholine groups significantly improved cytocompatibility [18,47,48,53] by modulating the

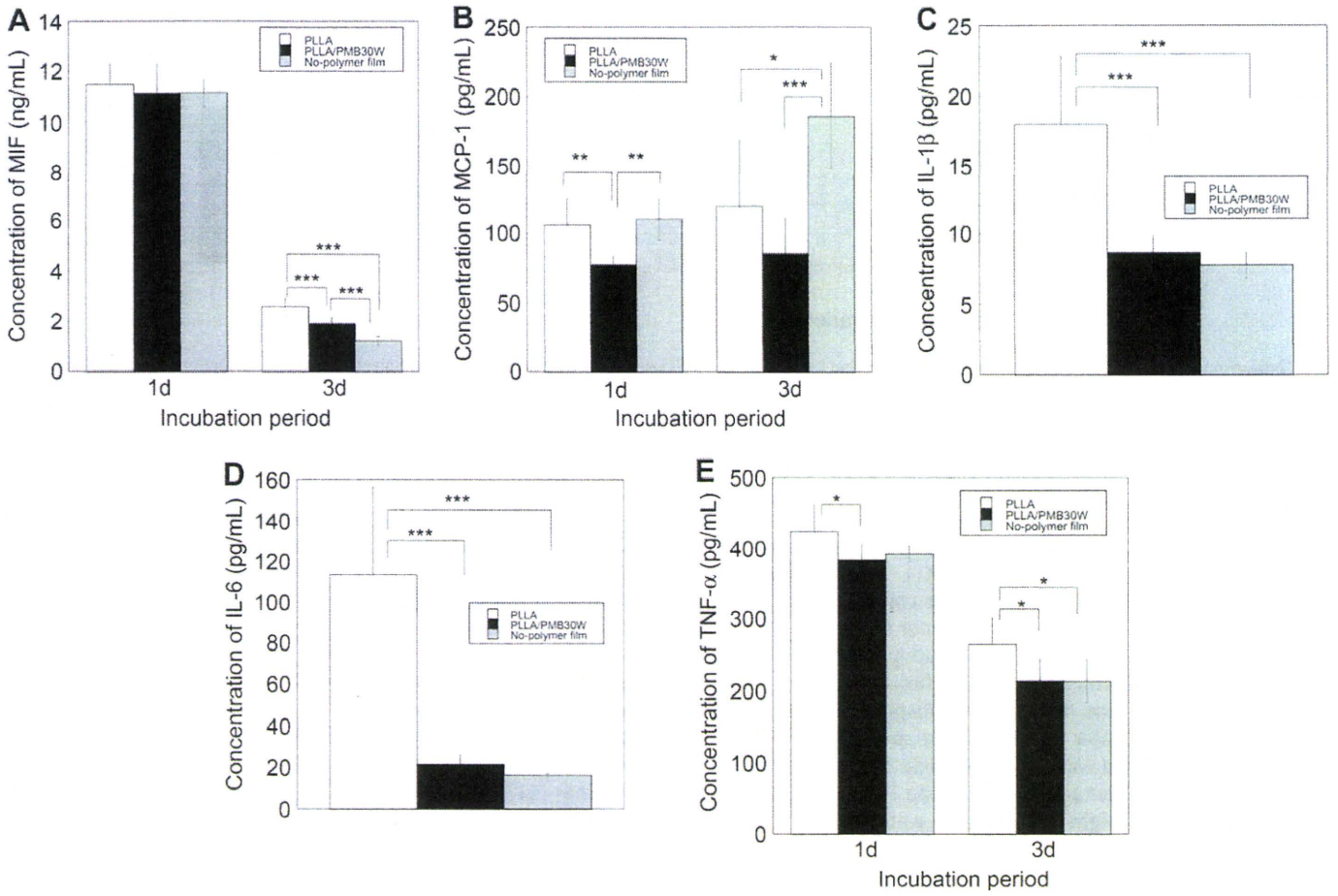

Fig. 6. Inflammatory cytokines released by human peripheral blood mononuclear cells. Data are presented as 8 cultures (PLLA and PLLA/PMB30W) and 7 cultures (No-polymer film). (A) MIF = macrophage migration inhibitory factor; (B) MCP-1 = monocyte chemoattractant protein-1; (C) IL-1β = interleukin 1β at 1 d; (D) IL-6 = interleukin 6 at 1 d; (E) TNF-α = tumor necrosis factor α. The *P* values were obtained by ANOVA with the Bonferroni correction.

leukocyte-mediated inflammatory reaction with monocyte quiescence. These findings strongly suggest that the homeostasis of human blood cells can be maintained by phosphorylcholine groups located on the surface of temporary cardiovascular stent materials.

4. Conclusion

Adverse tissue responses toward the PLLA used for temporary stenting were significantly reduced when the surface of the PLLA was covered with the phosphorylcholine groups by simple blending with an amphiphilic MPC copolymer, the PMB30W. In addition to temporary stenting eliminating the safety concerns involved in permanent cardiovascular stenting, the PLLA/PMB30W could reduce thrombotic occlusion under in vivo models and inflammatory reactions in vitro model. Therefore, we can believe that the PLLA/PMB30W is a promising material for temporary cardiovascular stent. A further investigation based on interventional procedures in large animal studies with long-term follow-up is necessary to confirm the clinical utility of these materials.

Acknowledgement

The authors are grateful for the helpful discussion and advice provided by Prof. Ung-Il Chung (The University of Tokyo). The assistance of the Global COE program in CMSI supported by the MEXT in Japan is acknowledged.

Appendix

Figures with essential color discrimination. Figs. 3 and 5 in this article are difficult to interpret in black and white. The full color images can be found in the online version, at doi:10.1016/j.biomaterials.2010.11.067.

Appendix. Supplementary data

Supplementary data associated with article can be found in online version at doi:10.1016/j.biomaterials.2010.11.067.

References

[1] Serruys PW, Kutryk MJ, Ong AT. Coronary-artery stents. N Engl J Med 2006;354:483–95.
[2] Mueller RL, Sanborn TA. The history of interventional cardiology: cardiac catheterization, angioplasty, and related interventions. Am Heart J 1995;129:146–72.
[3] Serruys PW, Ormiston JA, Onuma Y, Regar E, Gonzalo N, Garcia-Garcia HM, et al. A bioabsorbable everolimus-eluting coronary stent system (ABSORB): 2-year outcomes and results from multiple imaging methods. Lancet 2009;373:897–910.
[4] Ormiston JA, Serruys PW, Regar E, Dudek D, Thuesen L, Webster MW, et al. A bioabsorbable everolimus-eluting coronary stent system for patients with single de-novo coronary artery lesions (ABSORB): a prospective open-label trial. Lancet 2008;371:899–907.
[5] Tamai H, Igaki K, Kyo E, Kosuga K, Kawashima A, Matsui S, et al. Initial and 6-month results of biodegradable poly-l-lactic acid coronary stents in humans. Circulation 2000;102:399–404.

[6] van der Giessen WJ, Lincoff AM, Schwartz RS, van Beusekom HM, Serruys PW, Holmes Jr DR, et al. Marked inflammatory sequelae to implantation of biodegradable and nonbiodegradable polymers in porcine coronary arteries. Circulation 1996;94:1690–7.
[7] Schwartz RS, Holmes Jr DR, Topol EJ. The restenosis paradigm revisited: an alternative proposal for cellular mechanisms. J Am Coll Cardiol 1992;20:1284–93.
[8] Bergsma JE, de Bruijn WC, Rozema FR, Bos RR, Boering G. Late degradation tissue response to poly(L-lactide) bone plates and screws. Biomaterials 1995;16:25–31.
[9] Furie B, Furie BC. Mechanisms of thrombus formation. N Engl J Med 2008;359:938–49.
[10] Falati S, Gross P, Merrill-Skoloff G, Furie BC, Furie B. Real-time in vivo imaging of platelets, tissue factor and fibrin during arterial thrombus formation in the mouse. Nat Med 2002;8:1175–81.
[11] Kim HI, Takai M, Ishihara K. Bioabsorbable material-containing phosphorylcholine group-rich surfaces for temporary scaffolding of the vessel wall. Tissue Eng Part C Methods 2009;15:125–33.
[12] Ishihara K, Ueda T, Nakabayashi N. Preparation of phospholipid polymers and their properties as polymer hydrogel membrane. Polym J 1990;22:355–60.
[13] Ueda T, Oshida H, Kurita K, Ishihara K, Nakabayashi N. Preparation of 2-methacryloyloxyethyl phosphorylcholine copolymers with alkyl methacrylates and their blood compatibility. Polym J 1992;24:1259–69.
[14] Ishihara K. Novel polymeric materials for obtaining blood-compatible surfaces. Trends Polym Sci 1997;5:401–7.
[15] Ishihara K. Bioinspired phospholipid polymer biomaterials for making high performance artificial organs. Sci Technol Adv Mater 2000;1:131–8.
[16] Lewis AL. Phosphorylcholine-based polymers and their use in the prevention of biofouling. Colloids Surf B Biointerfaces 2000;18:261–75.
[17] Ishihara K, Goto Y, Takai M, Matsuno R, Inoue Y, Konno T. Novel polymer biomaterials and interfaces inspired from cell membrane functions. Biochim Biophys Acta, in press, doi:10.1016/j.bbagen.2010.04.008.
[18] Sawada S, Iwasaki Y, Nakabayashi N, Ishihara K. Stress response of adherent cells on a polymer blend surface composed of a segmented polyurethane and MPC copolymers. J Biomed Mater Res A 2006;79:476–84.
[19] Ishihara K, Shibata N, Tanaka S, Iwasaki Y, Nakabayashi N, Kurosaki T. Improved blood compatibility of segmented polyurethane by polymeric additives having phospholipid polar group. II. Dispersion state of the polymeric additive and protein adsorption on the surface. J Biomed Mater Res 1996;32:401–8.
[20] Hasegawa T, Iwasaki Y, Ishihara K. Preparation of blood-compatible hollow fibers from a polymer alloy composed of polysulfone and 2-methacryloyloxyethyl phosphorylcholine polymer. J Biomed Mater Res 2002;63:333–41.
[21] Long SF, Clarke S, Davies MC, Lewis AL, Hanlon GW, Lloyd AW. Controlled biological response on blends of a phosphorylcholine-based copolymer with poly(butyl methacrylate). Biomaterials 2003;24:4115–21.
[22] Ishihara K, Nomura H, Mihara T, Kurita K, Iwasaki Y, Nakabayashi N. Why do phospholipid polymers reduce protein adsorption? J Biomed Mater Res 1998;39:323–30.
[23] Kitano H, Imai M, Mori T, Gemmei-Ide M, Yokoyama Y, Ishihara K. Structure of water in the vicinity of phospholipid analogue copolymers as studied by vibrational spectroscopy. Langmuir 2003;19:10260–6.
[24] S. Chen, L. Li, C Zhao, J. Zheng. Surface hydration: principles and applications toward low-fouling/nonfouling biomaterials. Polymer 2010;51:5283–93.
[25] Ishihara K, Oshida H, Endo Y, Ueda T, Watanabe A, Nakabayashi N. Hemocompatibility of human whole blood on polymers with a phospholipid polar group and its mechanism. J Biomed Mater Res 1992;26:1543–52.
[26] Ishihara K, Ziats NP, Tierney BP, Nakabayashi N, Anderson JM. Protein adsorption from human plasma is reduced on phospholipid polymers. J Biomed Mater Res 1991;25:1397–407.
[27] Ishihara K, Aragaki R, Ueda T, Watanabe A, Nakabayashi N. Reduced thrombogenicity of polymers having phospholipid polar groups. J Biomed Mater Res 1990;24:1069–77.
[28] Snyder TA, Tsukui H, Kihara S, Akimoto T, Litwak KN, Kameneva MV, et al. Preclinical biocompatibility assessment of the EVAHEART ventricular assist device: coating comparison and platelet activation. J Biomed Mater Res A 2007;81:85–92.
[29] Yoneyama T, Sugihara K, Ishihara K, Iwasaki Y, Nakabayashi N. The vascular prosthesis without pseudointima prepared by antithrombogenic phospholipid polymer. Biomaterials 2002;23:1455–9.
[30] Yoneyama T, Ishihara K, Nakabayashi N, Ito M, Mishima Y. Short-term in vivo evaluation of small-diameter vascular prosthesis composed of segmented poly(etherurethane)/2-methacryloyloxyethyl phosphorylcholine polymer blend. J Biomed Mater Res 1998;43:15–20.
[31] Ishihara K, Iwasaki Y, Nakabayashi N. Polymeric lipid nanosphere consisting of water-soluble poly(2-methacryloyloxyethyl phosphorylcholine-co-n-butyl methacrylate). Polym J 1999;31:1231–6.
[32] Chin-Quee SL, Hsu SH, Nguyen-Ehrenreich KL, Tai JT, Abraham GM, Pacetti SD, et al. Endothelial cell recovery, acute thrombogenicity, and monocyte adhesion and activation on fluorinated copolymer and phosphorylcholine polymer stent coatings. Biomaterials 2010;31:648–57.
[33] Whelan DM, van der Giessen WJ, Krabbendam SC, van Vliet EA, Verdouw PD, Serruys PW, et al. Biocompatibility of phosphorylcholine coated stents in normal porcine coronary arteries. Heart 2000;83:338–45.
[34] Pinto Slottow TL, Waksman R. Overview of the 2007 food and drug administration circulatory system devices panel meeting on the endeavor zotarolimus-eluting coronary stent. Circulation 2008;117:1603–8.
[35] Kim HI, Takai M, Konno T, Matsuno R, Ishihara K. Biodegradable polymer films for releasing nanovehicles containing sirolimus. Drug Deliv 2009;16:183–8.
[36] Chuang TH, Stabler C, Simionescu A, Simionescu DT. Polyphenol-stabilized tubular elastin scaffolds for tissue engineered vascular grafts. Tissue Eng Part A 2009;15:2837–51.
[37] Therin M, Christel P, Li S, Garreau H, Vert M. In vivo degradation of massive poly(alpha-hydroxy acids): validation of in vitro findings. Biomaterials 1992;13:594–600.
[38] Sakai O, Nakayama Y, Nemoto Y, Okamoto Y, Watanabe T, Kanda K, et al. Development of sutureless vascular connecting system for easy implantation of small-caliber artificial grafts. J Artif Organs 2005;8:119–24.
[39] Garasic JM, Edelman ER, Squire JC, Seifert P, Williams MS, Rogers C. Stent and artery geometry determine intimal thickening independent of arterial injury. Circulation 2000;101:812–8.
[40] Sefton MV, Gemmell CH, Gorbet MB. What really is blood compatibility? J Biomater Sci Polym Ed 2000;11:1165–82.
[41] Williams DF. On the mechanisms of biocompatibility. Biomaterials 2008;29:2941–53.
[42] Boilard E, Nigrovic PA, Larabee K, Watts GF, Coblyn JS, Weinblatt ME, et al. Platelets amplify inflammation in arthritis via collagen-dependent microparticle production. Science 2010;327:580–3.
[43] Zernecke A, Bernhagen J, Weber C. Macrophage migration inhibitory factor in cardiovascular disease. Circulation 2008;117:1594–602.
[44] Jiang Y, Beller DI, Frendl G, Graves DT. Monocyte chemoattractant protein-1 regulates adhesion molecule expression and cytokine production in human monocytes. J Immunol 1992;148:2423–8.
[45] Ishii D, Schenk AD, Baba S, Fairchild RL. Role of TNF alpha in early chemokine production and leukocyte infiltration into heart allografts. Am J Transplant 2010;10:59–68.
[46] Brodbeck WG, Patel J, Voskerician G, Christenson E, Shive MS, Nakayama Y, et al. Biomaterial adherent macrophage apoptosis is increased by hydrophilic and anionic substrates in vivo. Proc Natl Acad Sci U S A 2002;99:10287–92.
[47] Sawada S, Sakaki S, Iwasaki Y, Nakabayashi N, Ishihara K. Suppression of the inflammatory response from adherent cells on phospholipid polymers. J Biomed Mater Res A 2003;64:411–6.
[48] DeFife KM, Yun JK, Azeez A, Stack S, Ishihara K, Nakabayashi N, et al. Adhesion and cytokine production by monocytes on poly(2-methacryloyloxyethyl phosphorylcholine-co-alkyl methacrylate)-coated polymers. J Biomed Mater Res 1995;29:431–9.
[49] Young TH, Lin DT, Chen LY. Human monocyte adhesion and activation on crystalline polymers with different morphology and wettability in vitro. J Biomed Mater Res 2000;50:490–8.
[50] Diaz-Guerra E, Vernal R, del Prete MJ, Silva A, Garcia-Sanz JA. CCL2 inhibits the apoptosis program induced by growth factor deprivation, rescuing functional T cells. J Immunol 2007;179:7352–7.
[51] Collier TO, Anderson JM, Brodbeck WG, Barber T, Healy KE. Inhibition of macrophage development and foreign body giant cell formation by hydrophilic interpenetrating polymer network. J Biomed Mater Res A 2004;69:644–50.
[52] Granchi D, Ciapetti G, Filippini F, Stea S, Cenni E, Pizzoferrato A, et al. In vitro cytokine production by mononuclear cells exposed to bone cement extracts. Biomaterials 2000;21:1789–95.
[53] Moro T, Takatori Y, Ishihara K, Konno T, Takigawa Y, Matsushita T, et al. Surface grafting of artificial joints with a biocompatible polymer for preventing periprosthetic osteolysis. Nat Mater 2004;3:829–36.